RAPID COMMUNICATION

Doping Mn into $(Li_{1-x}Fe_x)OHFe_{1-y}Se$ superconducting crystals via ion-exchange and ion-release/introduction syntheses*

Huaxue Zhou(周花雪)[1,2,†], Shunli Ni(倪顺利)[2,3,†], Jie Yuan(袁洁)[2,3], Jun Li(李军)[4], Zhongpei Feng(冯中沛)[2,3], Xingyu Jiang(江星宇)[2,3], Yulong Huang(黄裕龙)[2,3], Shaobo Liu(刘少博)[2,3], Yiyuan Mao(毛义元)[2,3], Fang Zhou(周放)[2,3], Kui Jin(金魁)[2,3], Xiaoli Dong(董晓莉)[2,3,‡], and Zhongxian Zhao(赵忠贤)[2,3]

[1] *College of Physics, Chongqing University, Chongqing* 401331, *China*
[2] *Beijing National Laboratory for Condensed Matter Physics, Institute of Physics, Chinese Academy of Science, Beijing* 100190, *China*
[3] *Key Laboratory for Vacuum Physics, University of Chinese Academy of Sciences, Beijing* 100049, *China*
[4] *Research Institute of Superconductor Electronics, Nanjing University, Nanjing* 210093, *China*

(Received 27 March 2017; published online 7 April 2017)

We report the success in introducing Mn into $(Li_{1-x}Fe_x)OHFe_{1-y}Se$ superconducting crystals by applying two different hydrothermal routes, ion exchange (1-step) and ion release/introduction (2-step). The micro-region x-ray diffraction and energy dispersive x-ray spectroscopy analyses indicate that Mn has been doped into the lattice, and its content in the 1-step fabricated sample is higher than that in the 2-step one. Magnetic susceptibility and electric transport properties reveal that Mn doping influences little on the superconducting transition, regardless of 1-step or 2-step routes. By contrast, the characteristic temperature T^*, at which the negative Hall coefficient reaches its minimum, is significantly reduced by Mn doping. This implies that the hole carriers contribution is obviously modified, and hence the hole band might have no direct relationship with the superconductivity in $(Li_{1-x}Fe_x)OHFe_{1-y}Se$ superconductors. Our present hydrothermal methods of ion exchange and ion release/introduction provide an efficient way for elements substitution/doping into $(Li_{1-x}Fe_x)OHFe_{1-y}Se$ superconductors, which will promote the in-depth investigations on the role of multiple electron and hole bands and their interplay with the high-temperature superconductivity in the FeSe-based superconductors.

Keywords: FeSe-based superconductors, doping, ion-exchange and release/introduction, Hall coefficient

PACS: 74.70.Xa, 82.30.Hk, 81.10.–h, 74.25.F– **DOI:** 10.1088/1674-1056/26/5/057402

1. Introduction

The newly discovered $(Li_{1-x}Fe_x)OHFe_{1-y}Se$ (FeSe-11111) superconductor has attracted extensive attention.[1–16] FeSe-11111 is composed by FeSe-tetrahedron layers and (Li/Fe)OH intercalation layers alternatively. Its superconducting transition temperature T_c, up to 43 K, is comparable with that of optimal $A_yFe_{2-x}Se_2$ compounds (A = alkeli metal),[17–22] and without the troublesome $\sqrt{5}\times\sqrt{5}$ Fe vacancy ordered insulating phase which is always intergrown with the superconductivity in FeSe-tetrahedron layers of $A_yFe_{2-x}Se_2$.[5] Besides, its electronic structure is quite similar to that of FeSe monolayer whose T_c is above 65 K.[9] The available high quality big single crystals together with its highly two-dimensional electron character.[6] ensure the FeSe-11111 system being propitious for unveiling the interplay of electronic anisotropy and high-T_c superconductivity in the multiband FeSe-based superconductors.

For in-depth investigations on the multiple electron and hole bands, especially their interplay with high-T_c superconductivity in FeSe-11111, the substitution of 3d metals on the Fe-sites should be an efficient method to tune the carrier density and the Fermi surface topology. In fact, the doping effect of Mn was widely studied in the Fe-based family,[23–29] and in some case, the Mn or other 3d elements that doped into the blocking layer do not work as a pair-breaking center, but rather modify the carriers or magnetic ordering.[29] In the FeSe-11111 system, however, the effects of 3d metal doping on the Fe-sites are still an open question.

In this work, we report that by applying ion exchange (1-step) and ion release/introduction (2-step) routes, manganese was successfully introduced, for the first time, into the lattice of $(Li_{1-x}Fe_x)OHFe_{1-y}Se$ single crystals. The superconductivity was not strictly suppressed by Mn doping, regardless of 1-step or 2-step samples. The negative Hall coefficient indicated that electron carriers dominate the electrical transport over the whole range of measuring temperature. The characteristic temperature T^*, at which the Hall coefficient reaches its minimum, is obviously reduced from about 130 K down to below 80 K, implying that the hole band might have no direct rela-

*Project supported by the National Natural Science Foundation of China (Grant Nos. 11574370 and 61501220), Frontier Program of the Chinese Academy of Sciences (Grant Nos. QYZDY-SSW-SLH001 and QYZDY-SSW-SLH008), the National Basic Research Program of China (Grant Nos. 2013CB921700 and 2016YFA0300301), and "Strategic Priority Research Program (B)" of the Chinese Academy of Sciences (Grant No. XDB07020100).

†These authors contributed equally.

‡Corresponding author. E-mail: dong@iphy.ac.cn

tionship with the superconductivity in $(Li_{1-x}Fe_x)OHFe_{1-y}Se$ superconductors.

2. Experiments

Figure 1 illustrates the syntheses process of Mn-doped (001)-orientated $(Li_{1-x}Fe_x)OHFe_{1-y}Se$ via two different hydrothermal routes, that is, the ion exchange (1-step) and ion release/introduction (2-step). All the hydrothermal reactions were performed in stainless steel autoclaves of 25 ml capacity with Teflon liners. The synthesis progress of 1-step was similar to that previous reported on the growth of $(Li_{0.84}Fe_{0.16})OHFe_{0.98}Se$ single crystal,[6] except that Mn powder was used as the starting material instead of Fe powder. The start materials of large $K_{0.8}Fe_{1.6}Se_2$ matrix crystal, 0.3 g Mn powder (Alfa Aesar, 99.95% purity), 4 g $LiOHH_2O$ (Alfa Aesar, 99.996% purity), and 0.003 mol selenourea (Alfa Aesar, 99.97% purity), were mixed with 5 ml de-ionized water and loaded into the autoclave, and then the autoclave was tightly sealed and heated at 100 °C for 72 h. The nominal $K_{0.8}Fe_{1.6}Se_2$ matrix crystal was synthesized via the same method described in the supplemental material of our previous work.[6] For the 2-step route, the synthesis progress consists of two parts, namely, the ion-release and ion-introduction. In the ion-release part, we used nominal $K_{0.8}Fe_{1.6}Se_2$ crystal as the matrix to obtain a large superconducting FeSe crystal of (001) orientation as introduced elsewhere.[30] The second progress was followed with the routine of 1-step but using FeSe crystal instead of $K_{0.8}Fe_{1.6}Se_2$. All the eventually obtained Mn-doped $(Li_{1-x}Fe_x)OHFe_{1-y}Se$ crystals were washed by de-ionized water for several times to remove soluble side products.

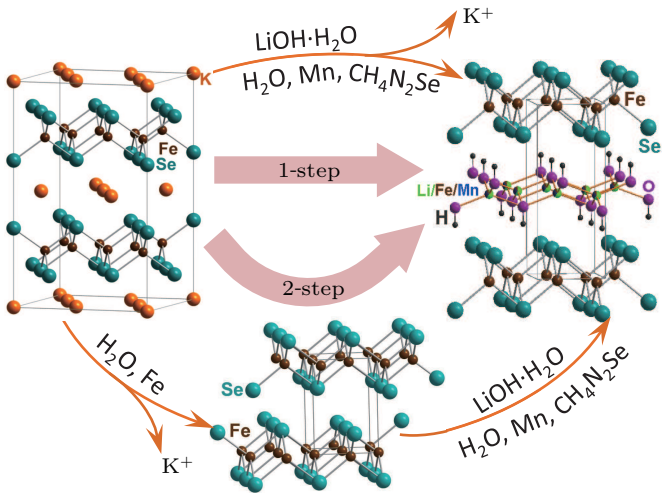

Fig. 1. Sketch of two different hydrothermal routes, ion exchange (1-step) and ion release/introduction (2-step).

X-ray diffraction (XRD) measurements of Mn-doped $(Li_{1-x}Fe_x)OHFe_{1-y}Se$ crystals were carried out at room temperature on a Rigaku SmartLab (9 kW) micro-region x-ray diffractometer with a ray source focusing 0.4 mm, with a 2θ range of 5°–80° and a scanning step of 0.02°. In order to check the chemical composition, both inductively coupled plasma atomic emission spectroscopy (ICP-AES) and energy dispersive x-ray spectroscopy (EDX) were carried out. The magnetic measurements were conducted on a Quantum Design MPMS-XL1 system with a measuring field of 1 Oe to characterize the superconducting state. Both in-plane electrical resistivity and Hall resistivity data were collected on a Quantum Design PPMS-9 T.

3. Result and discussion

The energy dispersive x-ray spectra are given in Figs. 2(a) and 2(b). The EDX analysis shows that Mn has been successfully doped into the crystal. Quantitatively analysis is conducted by applying the inductively coupled plasma atomic emission spectroscopy, which indicates that the atomic ratios of Mn:Fe:Se are (0.16:1.12:1) and (0.08:1.16:1) for the 1-step and 2-step samples, respectively. Consequently, the content of Mn in the 1-step sample is considerably larger than that in the 2-step sample.

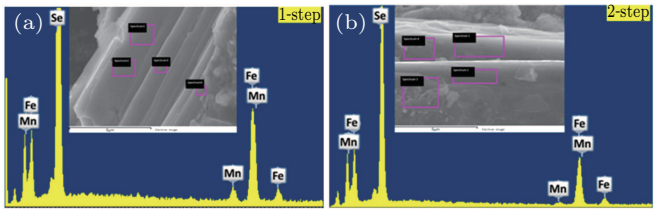

Fig. 2. EDX analysis for samples obtained from (a) 1-step and (b) 2-step routes, showing the presence of elements Fe, Mn, and Se. The insets show the corresponding SEM micrographs of the samples and regions where the data were collected.

Figure 3(a) shows the room temperature x-ray diffraction patterns of 1-step, 2-step, and Mn-free samples, demonstrating their crystal orientations along the (00l) planes. The corresponding c-axis lattice parameters are 9.272(3) Å, 9.306(3) Å, and 9.322(1) Å, respectively. The enlarged view of the (006) peak is shown in Fig. 3(b). With substitution of Mn, the (006) peaks show a pronounced rightward shift from the Mn-free $(Li_{0.84}Fe_{0.16})OHFe_{0.98}Se$. Considering the relatively smaller ion radius of Mn compared to that of Fe, it is reasonable to attribute the lattice shrink to the substitution of Mn onto the Fe-sites, which is also in agreement with the ICP results. To check the homogeneity of Mn doping, we also collected XRD data at 9 different areas within a width of 0.4 mm for the 1-step sample (Fig. 3(c)) and the 2-step sample (Fig. 3(d)). All the diffraction patterns are well consistent, without obvious peak shift.

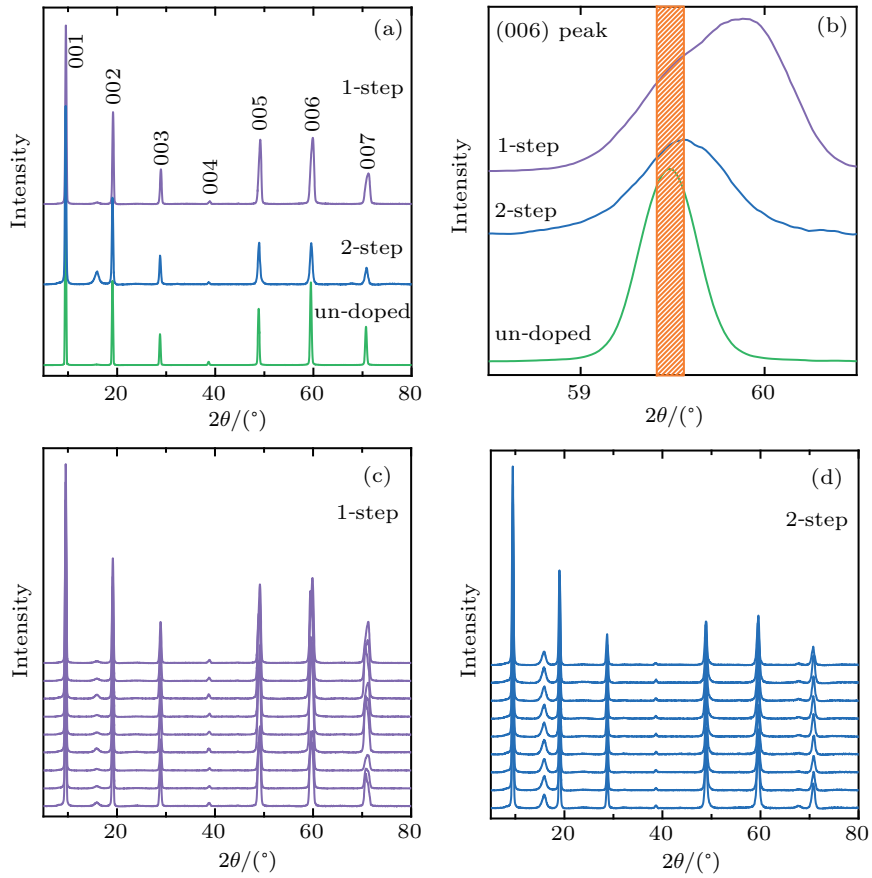

Fig. 3. (a) The XRD patterns of (00l) type for undoped $(Li_{0.84}Fe_{0.16})OHFe_{0.98}Se$ and Mn-doped $(Li_{1-x}Fe_x)OHFe_{1-y}Se$ crystals grown via ion exchange (1-step) and ion release/introduction (2-step). (b) Zoom-in (006) peaks, showing the position shift from left to right for 2-step and more remarkable for 1-step. (c) and (d) The XRD data collected uniformly in 9 different regions on the same sample for 1-step and 2-step samples, respectively.

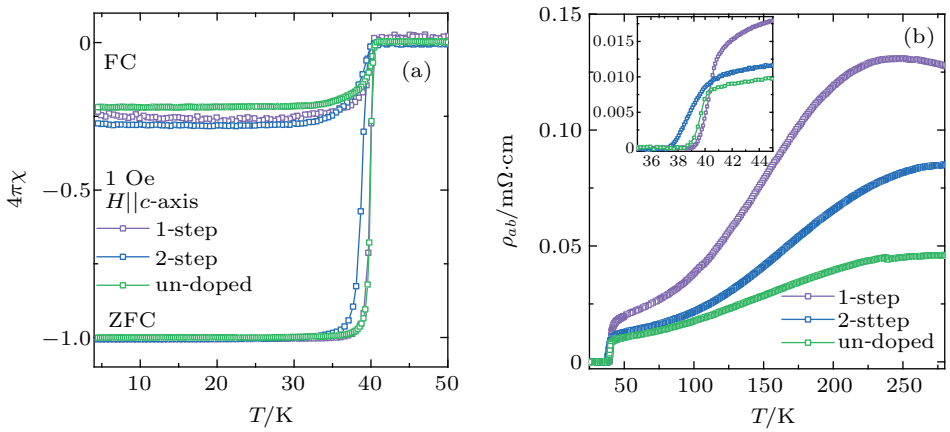

Fig. 4. (a) The magnetic susceptibilities of all crystals under zero-field cooling (ZFC) and field cooling (FC, H along the c-axis) show that sharp diamagnetic transitions occur at around 40 K for all samples. (b) Temperature dependence of in-plane resistivity for all crystals. The inset is the zoom-in view around the superconducting transition temperature.

The temperature dependence of the static magnetic susceptibility for Mn-free $(Li_{0.84}Fe_{0.16})OHFe_{0.98}Se$, 1-step and 2-step crystals exhibits a sharp diamagnetic transition. The onset T_c's for all crystals are almost identical ($\sim$ 40 K) with 100% diamagnetic shielding signal, as shown in Fig. 4(a). In Fig. 4(b), the temperature dependence of resistivity for the Mn-doped and Mn-free crystals shows that the zero resistance transition all occurs near 40 K as well. Obviously, the superconductivity of $(Li_{1-x}Fe_x)OHFe_{1-y}Se$ is not strongly sensitive to the Mn doping, being different from the previous results on other Fe-based superconductors.[23,24,26–29]

Actually, as shown in Fig. 5(a), the in-plane Hall resistivities (ρ_{xy}) for all crystals are also measured under the magnetic fields along the c-axis by sweeping the field up to 9 T at fixed temperatures. The extracted ρ_{xy} is proportional to the magnetic field at all measuring temperatures. The nega-

tive Hall coefficient (R_H) indicates that electron carriers dominate the electrical transport over the whole temperature range for all crystals (Fig. 5(b)). The Hall coefficient displays a minimum at a characteristic temperature T^*. As previously reported,[6] above T^*, the mobility of holes is reduced with decreasing temperature, leading to a decreasing Hall coefficient. Interestingly, the T^* is dramatically reduced from about 130 K (Mn-free crystal) down to below 80 K (1-step crystal, inset of Fig. 5(b)). This implies that the contribution of the hole carriers is obviously enhanced by Mn doping. Considering the fact that Mn doping shows no obvious influence on the superconductivity, we therefore suppose that the hole band has no direct relationship with the superconductivity in $(Li_{1-x}Fe_x)OHFe_{1-y}Se$ superconductors.

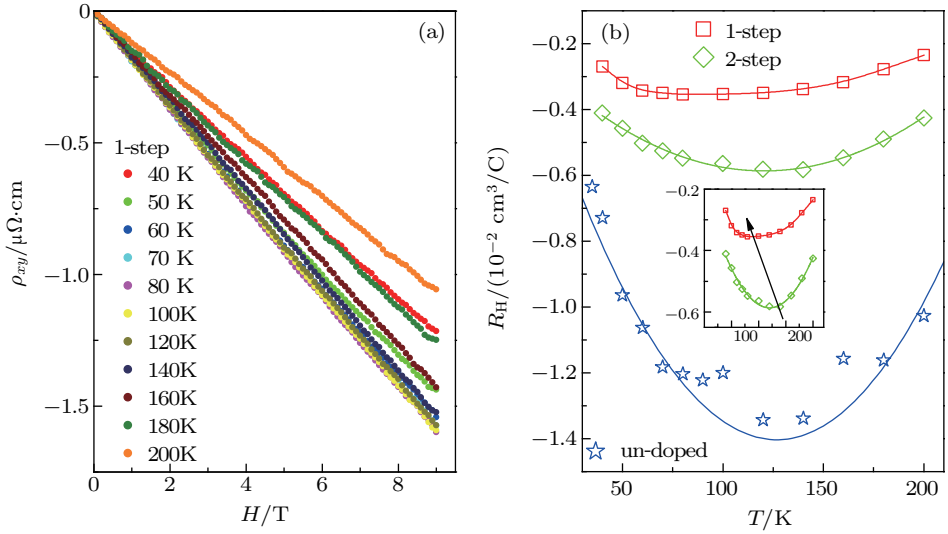

Fig. 5. (a) The Hall resistivity ρ_{xy} and (b) Hall coefficient R_H as a function of temperature for un-doped $(Li_{0.84}Fe_{0.16})OHFe_{0.98}Se$ and Mn-doped $(Li_{1-x}Fe_x)OHFe_{1-y}Se$ via 1-step and 2-step methods.

4. Conclusion

We have successfully doped Mn into $(Li_{1-x}Fe_x)OHFe_{1-y}Se$ crystal via both ion release/introduction and ion exchange. The Mn was found to be doped into the lattice structure by both methods, while the concentration of Mn in the 1-step fabricated sample is larger than that of 2-step. Magnetic susceptibility and electric transport properties indicate that Mn doping influences weakly on the superconducting transition, while the T^* is dramatically suppressed by Mn doping. It suggests that the hole band might have no direct relationship with the superconductivity in $(Li_{1-x}Fe_x)OHFe_{1-y}Se$ superconductors. Although we can hardly confirm the exact doping position of Mn on the superconducting layer or the block layer, the present results suggest that hydrothermal methods of ion release/introduction and ion exchange can provide an effective way to explore bulk functional crystals desired for both basic research and applications, particularly for the universal mechanism of high-T_c superconductivity.

References

[1] Lu X F, Wang N Z, Zhang G H, Luo X G, Ma Z M, Lei B, Huang F Q and Chen X H 2014 *Phys. Rev. B* **89** 020507R

[2] Lu X F, Wang N Z, Wu H, Wu Y P, Zhao D, Zeng X Z, Luo X G, Wu T, Bao W, Zhang G H, Huang F Q, Huang Q Z and Chen X H 2015 *Nat. Mater.* **14** 325

[3] Pachmayr U, Nitsche F, Luetkens H, Kamusella S, Brueckner F, Sarkar R, Klauss H H and Johrendt D 2015 *Angew. Chem. Int. Edit.* **54** 293

[4] Sun H, Woodruff D N, Cassidy S J, Allcroft G M, Sedlmaier S J, Thompson A L, Bingham P A, Forder S D, Cartenet S, Mary N, Ramos S, Foronda F R, Williams B H, Li X, Blundell S J and Clarke S J 2015 *Inorg. Chem.* **54** 1958

[5] Dong X, Zhou H, Yang H, Yuan J, Jin K, Zhou F, Yuan D, Wei L, Li J, Wang X, Zhang G and Zhao Z 2015 *J. Am. Chem. Soc.* **137** 66

[6] Dong X, Jin K, Yuan D, Zhou H, Yuan J, Huang Y, Hua W, Sun J, Zheng P, Hu W, Mao Y, Ma M, Zhang G, Zhou F and Zhao Z 2015 *Phys. Rev. B* **92** 064515

[7] Wu Y P, Zhao D, Lian X R, Lu X F, Wang N Z, Luo X G, Chen X H and Wu T 2015 *Phys. Rev. B* **91** 125107

[8] Khasanov R, Zhou H, Amato A, Guguchia Z, Morenzoni E, Dong X, Zhang G and Zhao Z 2016 *Phys. Rev. B* **93** 224512

[9] Zhao L, Liang A, Yuan D, Hu Y, Liu D, Huang J, He S, Shen B, Xu Y, Liu X, Yu L, Liu G, Zhou H, Huang Y, Dong X, Zhou F, Liu K, Lu Z, Zhao Z, Chen C, Xu Z and Zhou X J 2016 *Nat. Commun.* **7** 10608

[10] Du Z, Yang X, Lin H, Fang D, Du G, Xing J, Yang H, Zhu X and Wen H H 2016 *Nat. Commun.* **7** 10565

[11] Lei B, Xiang Z J, Lu X F, Wang N Z, Chang J R, Shang C, Zhang A M, Zhang Q M, Luo X G, Wu T, Sun Z and Chen X H 2016 *Phys. Rev. B* **93** 060501

[12] Yan Y J, Zhang W H, Ren M Q, Liu X, Lu X F, Wang N Z, Niu X H, Fan Q, Miao J, Tao R, Xie B P, Chen X H, Zhang T and Feng D L 2016 *Phys. Rev. B* **94** 134502

[13] Yu G, Zhang G Y, Ryu G H and Lin C T 2016 *J. Phys.: Condens. Matter* **28** 015701

[14] Zhou X, Borg C K H, Lynn J W, Saha S R, Paglione J and Rodriguez E E 2016 *Journal of Materials Chemistry C* **4** 3934

[15] Chen W, Zeng C, Kaxiras E and Zhang Z 2016 *Phys. Rev. B* **93** 064517

[16] Wang Z, Yuan J, Wosnitza J, Zhou H, Huang Y, Jin K, Zhou F, Dong X and Zhao Z 2017 *J. Phys.: Condens. Matter* **29** 025701

[17] Guo J G, Jin S F, Wang G, Wang S C, Zhu K X, Zhou T T, He M and Chen X L 2010 *Phys. Rev. B* **82** 180520

[18] Fang M H, Wang H D, Dong C H, Li Z J, Feng C M, Chen J and Yuan H Q 2011 *Europhys. Lett.* **94** 27009

[19] Yan Y J, Zhang M, Wang A F, Ying J J, Li Z Y, Qin W, Luo X G, Li J Q, Hu J P and Chen X H 2012 *Sci. Rep.* **2** 212

[20] Ying T P, Chen X L, Wang G, Jin S F, Lai X F, Zhou T T, Zhang H, Shen S J and Wang W Y 2013 *J. Am. Chem. Soc.* **135** 2951
[21] Zhang A M, Xia T L, Liu K, Tong W, Yang Z R and Zhang Q M 2013 *Sci. Rep.* **3** 1216
[22] Sedlmaier S J, Cassidy S J, Morris R G, Drakopoulos M, Reinhard C, Moorhouse S J, O'Hare D, Manuel P, Khalyavin D and Clarke S J 2014 *J. Am. Chem. Soc.* **136** 630
[23] Cheng P, Shen B, Hu J and Wen H H 2010 *Phys. Rev. B* **81** 174529
[24] Günther A, Deisenhofer J, Kant C, Nidda H A K v, Tsurkan V and Loidl A 2011 *Supercond. Sci. Tech.* **24** 045009
[25] Li J, Guo Y, Zhang S, Yuan J, Tsujimoto Y, Wang X, Sathish C, Sun Y, Yu S, Yi W, Yamaura K, Takayama-Muromachiu E, Shirako Y, Akaogi M and Kontani H 2012 *Phys. Rev. B* **85** 214509
[26] Singh S J, Shimoyama J, Yamamoto A, Ogino H and Kishio K 2013 *Physica C* **494** 57
[27] Zhou T T, Chen X L, Guo J G, Jin S F, Wang G, Lai X F, Ying T P, Zhang H, Shen S J, Wang S C and Zhu K X 2013 *J. Phys.: Condens. Matter* **25** 275701
[28] Deng Q, Ding X X, Li S, Tao J, Yang H and Wen H H 2014 *New J.Phys.* **16** 063020
[29] Li J, Guo Y F, Yang Z R, Yamaura K, Takayama-Muromachi E, Wang H B and Wu P H 2016 *Supercond. Sci. Tech.* **29** 053001
[30] Yuan D, Huang Y, Ni S, Zhou H, Mao Y, Hu W, Yuan J, Jin K, Zhang G, Dong X and Zhou F 2016 *Chin. Phys. B* **25** 077404R